University of New Hampshire
University of New Hampshire Scholars' Repository

Physics Scholarship | Physics

3-2015

Shock-induced prompt relativistic electron acceleration in the inner magnetosphere

J. C. Foster
Massachusetts Institute of Technology

J. R. Wygant
University of Minnesota - Twin Cities

M. K. Hudson
Dartmouth College

A. J. Boyd
University of New Hampshire - Main Campus

D. N. Baker
University of Colorado Boulder

See next page for additional authors

Follow this and additional works at: https://scholars.unh.edu/physics_facpub

 Part of the Astrophysics and Astronomy Commons

Recommended Citation

J. C. Foster, J. R. Wygant, M. K. Hudson, A. J. Boyd, D. N. Baker, P. J. Erickson, and H. E. Spence, 'Shock-induced prompt relativistic electron acceleration in the inner magnetosphere', Journal of Geophysical Research: Space Physics, vol. 120, no. 3, pp. 1661–1674, Mar. 2015.

This Article is brought to you for free and open access by the Physics at University of New Hampshire Scholars' Repository. It has been accepted for inclusion in Physics Scholarship by an authorized administrator of University of New Hampshire Scholars' Repository. For more information, please contact nicole.hentz@unh.edu.

Authors
J. C. Foster, J. R. Wygant, M. K. Hudson, A. J. Boyd, D. N. Baker, P. J. Erickson, and Harlan E. Spence

This article is available at University of New Hampshire Scholars' Repository: https://scholars.unh.edu/physics_facpub/346

AGU PUBLICATIONS

JGR

Journal of Geophysical Research: Space Physics

RESEARCH ARTICLE
10.1002/2014JA020642

Special Section:
New perspectives on Earth's radiation belt regions from the prime mission of the Van Allen Probes

Key Points:
- Dual-spacecraft dayside observations quantify shock-induced effects
- Drift resonance with induced electric fields accelerates 3–4 MeV electrons
- Energy increase ~500 keV occurs in <20 min for 3 MeV at L^*~3.8

Correspondence to:
P. J. Erickson,
pje@haystack.mit.edu

Citation:
Foster, J. C., J. R. Wygant, M. K. Hudson, A. J. Boyd, D. N. Baker, P. J. Erickson, and H. E. Spence (2015), Shock-induced prompt relativistic electron acceleration in the inner magnetosphere, *J. Geophys. Res. Space Physics*, *120*, 1661–1674, doi:10.1002/2014JA020642.

Received 21 SEP 2014
Accepted 8 JAN 2015
Accepted article online 10 JAN 2015
Published online 9 MAR 2015

Shock-induced prompt relativistic electron acceleration in the inner magnetosphere

J. C. Foster[1], J. R. Wygant[2], M. K. Hudson[3], A. J. Boyd[4], D. N. Baker[5], P. J. Erickson[1], and H. E. Spence[4]

[1]Haystack Observatory, Massachusetts Institute of Technology, Westford, Massachusetts, USA, [2]Department of Physics and Astronomy, University of Minnesota, Minneapolis, Minnesota, USA, [3]Physics and Astronomy Department, Dartmouth College, Hanover, New Hampshire, USA, [4]Institute for the Study of Earth, Oceans, and Space, University of New Hampshire, Durham, New Hampshire, USA, [5]Laboratory for Atmospheric and Space Physics, University of Colorado Boulder, Boulder, Colorado, USA

Abstract We present twin Van Allen Probes spacecraft observations of the effects of a solar wind shock impacting the magnetosphere on 8 October 2013. The event provides details both of the accelerating electric fields associated with the shock and the response of inner magnetosphere electron populations across a broad range of energies. During this period, the two Van Allen Probes observed shock effects from the vantage point of the dayside magnetosphere at radial positions of $L = 3$ and $L = 5$, at the location where shock-induced acceleration of relativistic electrons occurs. The extended (~1 min) duration of the accelerating electric field across a broad extent of the dayside magnetosphere, coupled with energy-dependent relativistic electron gradient drift velocities, selects a preferred range of energies (3–4 MeV) for the initial enhancement. Those electrons—whose drift velocity closely matches the azimuthal phase velocity of the shock-induced pulse—stayed in the accelerating wave as it propagated tailward and received the largest increase in energy. Drift resonance with subsequent strong ULF waves further accentuated this range of electron energies. Phase space density and positional considerations permit the identification of the source population of the energized electrons. Observations detail the promptness (<20 min), energy range (1.5–4.5 MeV), energy increase (~500 keV), and spatial extent (L^* ~3.5–4.0) of the enhancement of the relativistic electrons. Prompt acceleration by impulsive shock-induced electric fields and subsequent ULF wave processes therefore comprises a significant mechanism for the acceleration of highly relativistic electrons deep inside the outer radiation belt as shown clearly by this event.

1. Introduction

Understanding the processes that cause the energization of radiation belt particles to relativistic energies is a prime objective of NASA's Van Allen Probes mission [*Mauk et al*., 2012]. During both disturbed and more quiescent conditions, the population of outer radiation belt electrons is affected by multiple processes, and the Van Allen Probes mission has to date made significant advances in our understanding of the characteristics of these processes [*Baker et al*., 2013; *Turner et al*., 2014]. *Baker et al*. [2014] contrasted the gradual effects of slow inward diffusion with impulsive events that can produce drastic losses, energization, and reconfiguration. *Reeves et al*. [2013] presented evidence for storm time local acceleration of electrons to relativistic energies in the core regions of the outer zone, and *Thorne et al*. [2013] developed a theoretical description of that acceleration process in terms of resonant interaction with whistler mode waves. *Foster et al*. [2014] described the role of impulsive substorm processes in providing both the seed population of energetic electrons and the wave amplification required for in situ prompt acceleration of energetic electrons to highly relativistic energies.

In this paper we present direct experimental observations of the effects of a solar wind shock impacting the magnetosphere, providing a significant mechanism for prompt acceleration of electrons to highly relativistic energies in the inner magnetosphere. The twin Van Allen Probes spacecraft provide detailed observations both of the accelerating electric fields associated with the shock impulse and the response of inner magnetosphere electron populations across a broad range of energies.

A crucial feature of the present study is the observation of the shock encounter from the vantage point of the dayside magnetosphere by the two Van Allen Probes at radial positions of $L = 3$ and $L = 5$, at the location where abrupt shock-induced acceleration of relativistic electrons occurs. By contrast, previous observations

©2015. American Geophysical Union. All Rights Reserved.

of shock acceleration with the Combined Release and Radiation Effects Satellite (CRRES) [*Blake et al*., 1992; *Wygant et al*., 1994] were obtained on the nightside of Earth's magnetosphere. The simultaneous dayside observations at two different locations provide strong evidence of the spatial extent and duration of the shock-induced electric field along with the spatial regions over which acceleration took place. Van Allen Probe observations from the Relativistic Electron-Proton Telescope (REPT) instrument [*Baker et al*., 2012] further allow the identification of the source population of the energized electrons, along with crucial information such as phase space density and position relative to the energized population. Finally, the Van Allen Probes relativistic particle detectors' energy and pitch angle resolution allow for the first time a direct assessment of the energy of the particles that are the most efficiently accelerated. During a shock encounter that conserves the first and second adiabatic invariants, but which violates the third invariant, application of Liouville's theorem indicates that the phase space density of both the source population and energized population should be conserved along a phase space trajectory. This allows us to identify with a high level of confidence the original position of the source population and to assess whether the measured electric fields can effectively inject and energize the source electrons to form the energized population.

Previous work modeled various aspects of the dramatic effects of a strong solar wind shock on the radiation belt. The CRRES observations of the March 1991 shock acceleration event reported by *Blake et al*. [1992] were the most remarkable. *Wygant et al*. [1994] described in detail the in situ electric and magnetic field measurements by CRRES and estimated the characteristics of the accelerated particles produced. *Li et al*. [1993] and *Elkington et al*. [2002] examined and modeled electron acceleration as the shock-induced magnetosonic impulse propagated into the magnetosphere. The extensive radiation belt perturbations associated with the October–November 2003 multiple shock events and storms were well observed by the low-altitude polar-orbiting SAMPEX satellite [*Baker et al*., 2004] and modeled using MHD test particle simulations [*Kress et al*., 2007]. Prior investigations examined the impulsive acceleration of the preexisting population of MeV electrons to higher energies via interaction with the azimuthal electric field impulse that accompanies magnetopause compression. Other work examined the subsequent effects of drift-resonant acceleration by "ringing" ULF electric field oscillations that follow the initial shock impulse (see *Hudson et al*. [1997] and *Hudson et al*. [2004] for CRRES observations, *Zong et al*. [2009] for Cluster observations, and *Eriksson et al*. [2006] for a summary of earlier observations). Such effects are implicitly included in MHD test particle simulation studies. Persistent coherent ULF oscillations over hours following a coronal mass ejection (CME) shock are a resonant mode of the system and are potentially a consequence of continued strong solar wind forcing [*Tan et al*., 2011; *Claudepierre et al*., 2013; *Mann et al*., 2013].

For the March 1991 highly relativistic (15 MeV) event seen by CRRES, the energization from 5 to 15 MeV follows from first invariant conservation and inward transport of a multi-MeV electron source population from L~7 to $L = 2.6$ over a fraction of an electron drift period. The resonant electron population gradient-curvature drifts at a velocity comparable to the fast-mode speed of the azimuthal electric field impulse such that the electrons see an approximately constant electric field in their frame of reference. This magnetosonic electric field impulse was also inferred by other spacecraft and ground magnetometer measurements to be propagating azimuthally at approximately the fast-mode speed [*Araki et al*., 1997], matching results from MHD simulations of such events [*Kress et al*., 2007]. In particular, *Wygant et al*. [1994] estimated an initial azimuthal electric field amplitude of ~200 mV/m on the dayside (CRRES observations were made at 22:00 magnetic local time (MLT) on the nightside). We note that this intense inferred dayside impulse is comparable to that seen in MHD simulations for the Halloween 2003 storm [*Kress et al*., 2007] and is larger by an order of magnitude than the measured dayside impulse during the 8 October 2013 event reported herein.

We summarize in this study the multipoint observations from the 8 October 2013 event and discuss at a heuristic level the physical mechanisms involved in the shock acceleration and its aftermath. The 8 October event represents a moderate solar wind shock at a time when the Van Allen Probe spacecraft (A and B) were inside the low-energy plasmasphere on the dayside of the magnetosphere. Both spacecraft were within the well-developed outer radiation belt, containing an enhanced relativistic electron population due to a disturbance several days earlier. The 8 October event is thus distinct from the March 1991 event, particularly in the availability of measurements from spacecraft in the upstream interplanetary medium, allowing determination of solar wind input parameters and shock properties driving the observed acceleration event. These additional observations provide a crucial boundary condition on the chain of events that ensued.

©2015. American Geophysical Union. All Rights Reserved.

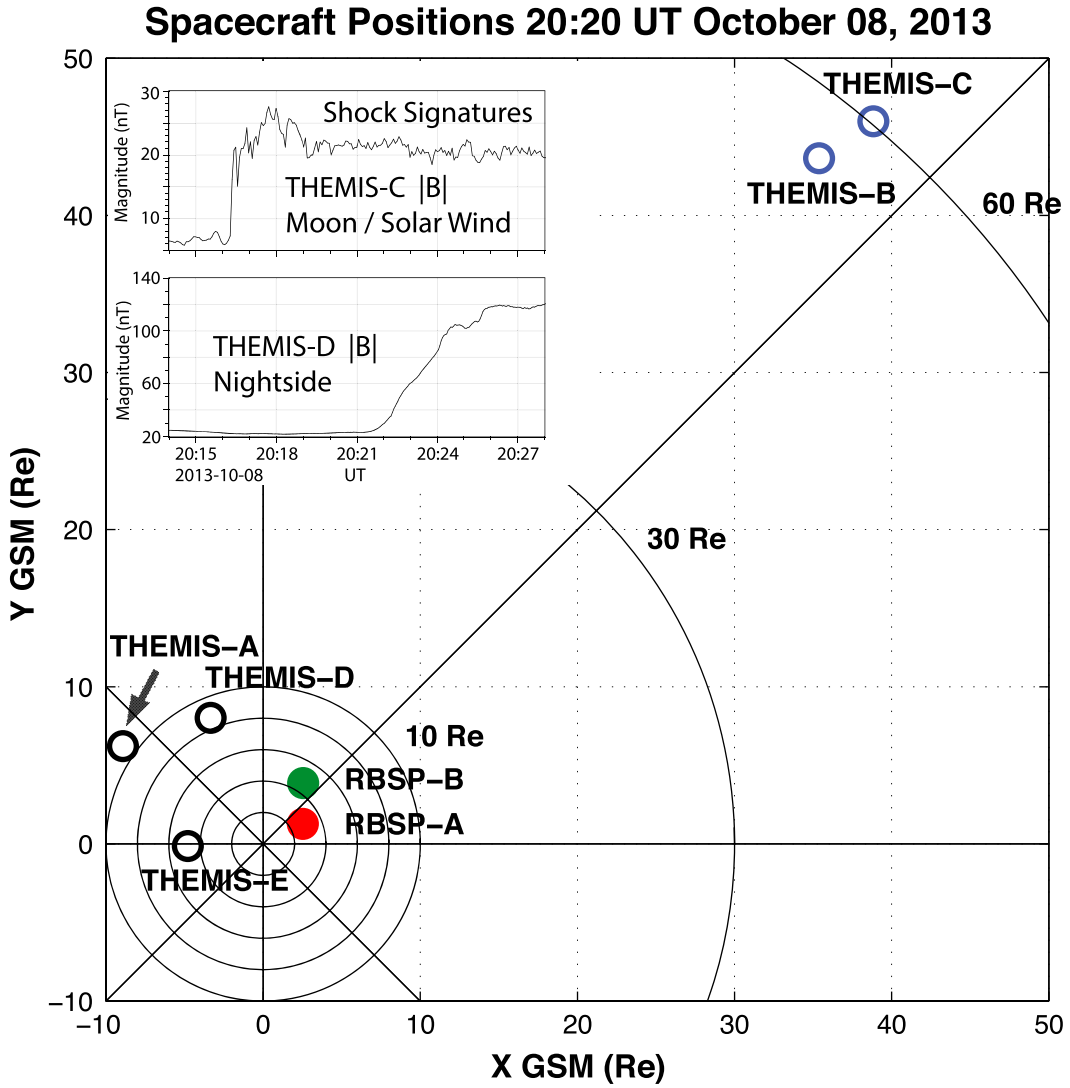

Figure 1. Equatorial plane positions are shown in GSM coordinates (*X* directed toward the Sun) for the two Van Allen Probes in the inner magnetosphere on the dayside, the two ARTEMIS spacecraft (i.e., THEMIS B and C) orbiting the Moon in the solar wind, and the THEMIS A, D, and E spacecraft on the dusk flanks in the magnetosphere. The inset shows the magnetic signature of the interplanetary shock in the solar wind (THEMIS C) and of the shock-induced magnetosonic impulse in the nightside magnetosphere (THEMIS D).

2. Observations

2.1. Shock Observations

Figure 1 shows the equatorial plane position of the two Van Allen Probes in the inner magnetosphere on the dayside; the two ARTEMIS spacecraft (i.e., Time History of Events and Macroscale Interactions during Substorms (THEMIS) B and C) orbiting the Moon in the solar wind; and the THEMIS A, D, and E spacecraft on the dusk flanks in the magnetosphere. (The availability of the ARTEMIS data for this event is critical because of a dropout in OMNI data from the ACE and Wind spacecraft during the time of shock arrival.) The inset provides measurements of the interplanetary shock and its magnetic signature in the solar wind (THEMIS C) and nightside magnetosphere (THEMIS D). Figure 2 presents the measurements of the shock-induced electric field signature in the dayside inner magnetosphere as observed by the Van Allen Probes. The shock in the interplanetary medium was first seen by the two ARTEMIS spacecraft at about 20:16:20 UT (inset of Figure 1). These spacecraft were orbiting the Moon at about 60 R_E geocentric distance in the upstream solar wind at ~15 MLT. About 5 min later (20:21:25 UT), Figure 2 shows that Van Allen Probe A observed a strong electric field enhancement (~12 mV/m) in the dayside magnetosphere, followed ~20 s later by a similar signal in Van

©2015. American Geophysical Union. All Rights Reserved.

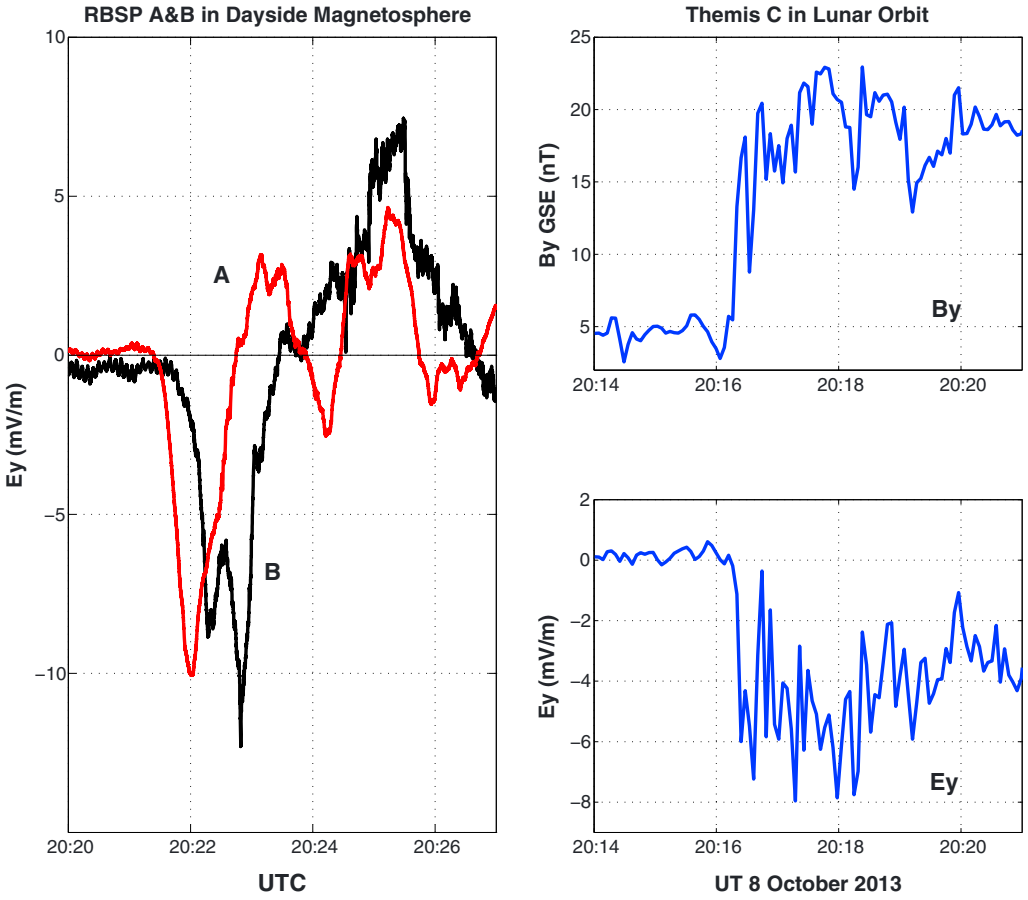

Figure 2. (left) The shock-induced electric field signatures ($V_{SC} \times B$ subtracted) in the dayside inner magnetosphere as observed by the Van Allen Probes. (right) The shock in the interplanetary medium was seen by the two ARTEMIS spacecraft at about 20:16:20 UT. Probe A observed a strong electric field enhancement (~12 mV/m), followed ~20 s later by a similar signal at Probe B (20:21:45 UT).

Allen Probe B (20:21:45 UT). At each probe, the electric field signature was associated with an increase in the magnetic field magnitude of ~40 nT (not shown) over an ~60 s time span.

We interpret these observations as evidence that the bipolar electric field signature of magnetopause compression observed inside the magnetosphere was the consequence of an encounter with the interplanetary shock. In the interplanetary medium (THEMIS C), the time scale for the increase in the magnetic field at the magnetic ramp was at or below the ARTEMIS instrument sample cadence of 6 s. However, the magnetic ramp and induced electric field in the dayside inner magnetosphere observed by the Van Allen Probes were seen to be on the order of 40–100 s, spanning many sample periods. This longer time scale can be explained by the characteristic time scale of the piston-like compression of the magnetosphere by the interplanetary shock and the consequent launching of a fast-mode wave into the magnetosphere. We can qualitatively estimate this time scale as the ratio of the spatial scale of the magnetic dipole radial gradient in the equatorial plane at the point of maximal compression ($L_S \sim B/\nabla|B| \sim R/3 \sim 8/3\ R_E$) and the velocity of the shock compression (V_c). We take V_c to be the fast-mode speed ~450 km/s as determined by local plasma parameters at the spacecraft (see section 2). Thus, the time scale for compression is $T \sim (8/3)\ R_E/V_c \sim 40$ s, in good agreement with the in-situ Van Allen Probe observations. (A more precise estimate can be derived in future studies using global MHD simulations.)

At the time of the shock-driven wave encounter, Van Allen Probe B was located at $L = 5$, MLT = 17.3, with a magnetic latitude (MLAT) = 14°. Van Allen Probe A was located further inside the magnetosphere at $L = 3$, MLT = 13.5, and MLAT = 16.3°. The Probe B position vector was R_B = (16,500, 21,500, 15,000) km in a geocentric

©2015. American Geophysical Union. All Rights Reserved.

ecliptic coordinate system (GSE), while the Probe A position vector was $R_A = (16{,}000, 6000, 7000)$ km GSE. It is noteworthy that the X_{GSE} (sunward) positions of the two spacecraft were nearly identical and that the total separation of Probe A and Probe B was 17,450 km and was nearly all in the Y_{GSE} direction (approximately azimuthal at this location). The negative pulses in the electric field lasted on the order of 60 s, and the time delay between the signals observed by the two spacecraft was on the order of 20 s with Probe A, at a smaller radial distance, observing the signal first. This strongly suggests that the pulse was propagating azimuthally in the prenoon to postnoon direction. Total propagation velocity between Probes A and B (17,450 km/20 s) was ~850 km/s. The pulse propagation speed is important in determining the energy of electrons that drift in resonance with an impulse propagating azimuthally at the fast-mode speed.

2.2. Shock Interpretation

In most simple scenarios, a shock impacting the subsolar point of the magnetosphere drives the magnetopause earthward in a piston-like motion that launches a fast-mode wave that propagates both radially inward (earthward) and azimuthally around the Earth [*Araki et al.*, 1997; *Gannon et al.*, 2005]. The local fast-mode speed can be estimated from Van Allen Probe spacecraft measurements of in situ magnetic field and density. At the time of shock pulse encounter, both spacecraft were in the high-density plasmasphere. Probe B, at $L = 5$, measured a local magnetic field of ~300 nT with density ~200 cm^{-3}. The temperature is not directly measured, but characteristic thermal energy in the plasmasphere is ~1 eV. Thus, the fast-mode speed is on the order of 450 km/s in the appropriate cold plasma limit. Probe A, at $L = 3$, measured a local density of 1500 cm^{-3} and a local magnetic field of 1500 nT, resulting in a fast-mode speed of 715 km/s. The observed total propagation speed (~850 km/s) is quite comparable to these estimates of the fast-mode velocity. The difference between the fast-mode speed ~500 km/s and the azimuthal phase velocity of the shock-induced pulse (~850 km/s) can be due to the obliquity of the phase front normal vector to a (local) azimuthally directed vector. An obliquity angle of 30° could account for the observed difference.

The measurements from the two spacecraft provide evidence that a substantial portion of the dayside equatorial magnetosphere was occupied for periods of 1–2 min with a strong dusk-dawn/azimuthal component of the electric field. This component is of special interest because charged particles that drift azimuthally as a consequence of the gradient and curvature drifts in the Earth's magnetic field will traverse this electric field, acquiring significant amounts of energy.

In general, a lower energy charged particle on the dayside drifting comparatively slowly within the Earth's magnetic field will encounter the shock-induced electric fields over a time scale set by the duration of the shock electric field presence on the dayside. A higher (lower) energy particle may drift across the dayside on a time scale shorter (longer) than the time scale for the existence of the electric field on the dayside. Finally, as the wavefront associated with the accelerating electric fields expands azimuthally around the magnetosphere to the nightside, some "resonant" particles may drift at nearly the same velocity as the front and through a resonant interaction experience the electric field for a longer period of time [*Kress et al.*, 2007].

For example, if the electric field is present over the entire spatial extent from 09:00 MLT to 15:00 MLT at $L = 4$, a distance of about 6 R_E in the equatorial plane, it will traverse an electric potential of ~6 $R_E \times 6400$ km/$R_E \times 12$ mV/m ~38,000 km × 12 mV/m~400 kV. This estimate provides a broad constraint on the maximum amount of energy any particle can obtain traversing the region of strong electric field. Only particles with sufficient perpendicular energy to drift across the dayside over a period of 1–2 min or faster can obtain this energy. This corresponds to a perpendicular energy of 3–4 MeV at $L = 4$.

Figure 3 presents the energy dependence of the relativistic electron drift period for a range of L values, following the method of *Schulz and Lanzerotti* [1974]. For comparison with the shock impulse propagation speed inside the magnetosphere ~850 km/s estimated above, a 3.6 MeV electron at $L = 5$ has a 235 s drift period which corresponds to a 855 km/s azimuthal velocity V_ϕ:

$$V_\phi(3.6\ \text{MeV}) = 2\pi\ 5\ R_E(R_E = 6400\ \text{km})/235\ \ \text{s} = 855\ \text{km/s}$$

In considering the energization of drift-resonant electrons, the value of the $E \times B$ drift of the particles in the wavefields provides important information. The $E \times B$ drift is $\delta E \times B/B^2$~12 mV/m/280 nT = ~40 km/s at spacecraft B and ~20 km/s at spacecraft A. Therefore, if an electron encounters these fields for a period of

©2015. American Geophysical Union. All Rights Reserved.

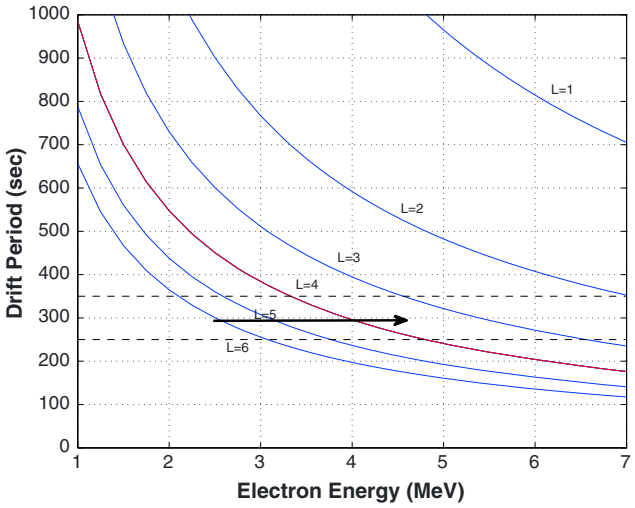

Figure 3. The energy dependence of the relativistic electron drift period for a range of dipole L values is shown. For comparison with the estimated ~850 km/s shock impulse propagation speed inside the magnetosphere, a 3.6 MeV electron at $L = 5$ has a 235 s drift period which corresponds to a 855 km/s azimuthal velocity. The 2.5 MeV electrons resonant with ULF waves with ~300 s period at L~6 and experiencing $E_y < 0$ on the dayside will be energized and displaced inward. For strong enough ULF waves, the heavy black arrow indicates the increasing energy of an electron that remains in resonance with the wave as the electron moves radially inward (see discussion in section 2.2).

100 s, then it will drift earthward by $\delta R = 2000–4000$ km = 0.3 to 0.6 R_E. This implies that the source population for the acceleration process should be at a radial distance 0.3 R_E (Probe A) to 0.6 R_E (Probe B) larger than the spacecraft position at the time of appearance of the energized electron population. While the minimum time scale for the interaction of an electron with the shock-induced pulse (T_{pulse}) is ~60 s (cf., Figure 2), the bounce period (T_b) of a 3 MeV electron at $L = 4.5$ ranges from 0.5 s to 0.25 s for pitch angles between 0 and 90°, and the drift period (T_d) is ~250 s. Since $T_b \ll T_{pulse} < T_d$, both the first and second adiabatic invariants are conserved in the interaction, while the third invariant is broken. Thus, the source population should have the same phase space density as the energized population for the same first and second invariants.

We conclude from these analyses of the impulse propagation that ~4 MeV electrons would be preferentially accelerated in the L~4–5 region of the electron observations described in the next section. Additionally, we would expect the source population to be ~0.3 R_E beyond the energized population and expect a maximum energization of ~400 keV. We show observationally below (e.g., Figure 7) that just such a source population exists, with the same phase space density as the energized population of 4 MeV electrons at L^* ~4.0. L^* is inversely proportional to the third adiabatic invariant or the magnetic flux through a drift orbit [*Roederer*, 1970]. L^* is not conserved in the shock impulse interaction. In this paper L^* is calculated using the *Tsyganenko and Sitnov* [2005] magnetic field model.

2.3. Relativistic Electron Observations

Figure 4 shows the relativistic electron flux increases in the 3.6 MeV channel from the REPT instrument [*Baker et al*., 2012] on the Van Allen Probes A and B at about 20:22 UT on 8 October 2013. Figure 4 (bottom) presents the measurements of color-coded electron flux in the 3.6 MeV REPT channel as a function of pitch angle (vertical scale) and time (horizontal scale) from each of the two probes. The shock-driven electric field at each spacecraft is included in Figure 4 (top) for reference purposes. The measurements from Probe B show relativistic electron drift echoes with a regular periodicity on the order of 350–400 s. In particular, the drift echoes observed by Probe B are characterized by "quasiperiodic pulse-like" enhancements in the relativistic flux by about an order of magnitude and are a consequence of prompt energization of electrons due to the shock-induced fields on a time scale that is a fraction of the orbital drift period around the Earth. At least six such echoes are observed. The periodicity in the pulse corresponds to the drift period of a 3.6 MeV electron around the Earth at $L = 5$ due to the gradient B and curvature drift in the Earth's dipole magnetic field (see Figure 3).

Relativistic electron drift echoes are also observed by Probe A. Despite the similarities in the electric field amplitude and duration observed by Probe A, the intensity of the fluxes in the initial drift echoes observed by Probe A are much less than those observed by Probe B. As Probe A moved outward along its orbit by 1–2 R_E over the next 15 min, it encountered the region of strongest electron acceleration at L~4 (cf., Figure 6) and observed 3–4 drift echoes with about the same intensity as those more promptly observed at L~5 by Probe B.

©2015. American Geophysical Union. All Rights Reserved.

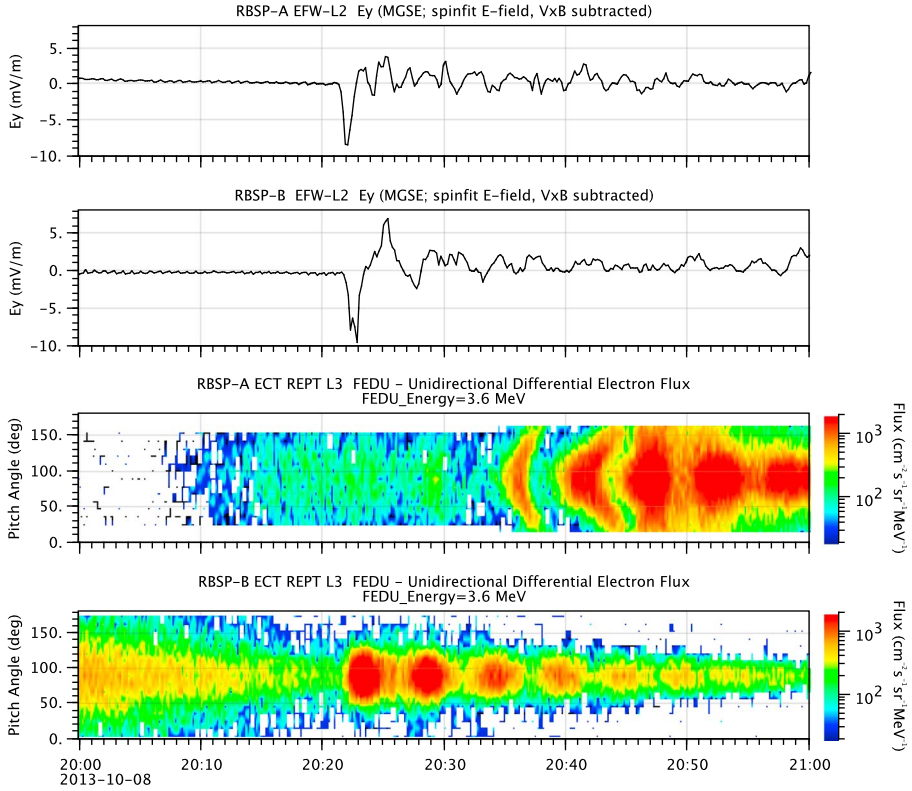

Figure 4. Relativistic electron flux increases in the 3.6 MeV channel from the REPT instrument on Van Allen Probes A and B is shown. (top) The shock-driven electric field at each spacecraft is included for reference. (bottom) Measurements of electron flux in the 3.6 MeV REPT channel are shown as functions of pitch angle and time from each of the two probes.

The duration (full width at half maximum) of the pulse of energized electrons observed by Probe A at 90° pitch angle in the 3.6 MeV channel, coincident with the shock impulse, is 40%–50% of the measured drift period of that electron energy at $L^* = 3.8\ R_E$. This implies that the acceleration event occurred over a significant fraction of a drift path, consistent with acceleration over a large portion of the dayside magnetopause. If we define the fractional increase in energy of a particle as the kinetic energy KE_F gained divided by the initial kinetic energy KE_0; i.e., $(KE_F - KE_0)/KE_0 \sim \delta KE/KE_0$, the particles that gain the greatest fractional increase in kinetic energy are those that spend the longest time in the accelerating electric fields. Higher-energy electrons (>3.6 MeV) will drift through the dayside region of strong shock electric fields on a time scale much faster than the 60–100 s duration of the magnetosonic impulse electric field. Such particles are likely to see an upper bound on their acceleration set by the azimuthal amplitude of the electric field (E) times its azimuthal spatial scale, or $\int E \cdot d_s \sim$250–500 keV. This estimate of the maximum expected energization compares well with that estimated from the adiabatic energy change due to the inward displacement of the electrons (400 keV) described in section 2b.

In Figure 5, we present the energy and temporal extent of the relativistic electron drift echoes observed by Van Allen Probe A across several discrete detector channels. We note significant shock response and drift echoes across a two-decade electron energy range interval of 50 keV to >5 MeV, as determined by combined Magnetic Electron Ion Spectrometer (MagEIS) [*Blake et al.*, 2013] and REPT observations from the Van Allen Probe Energetic particle, Composition, and Thermal plasma instrument suite [*Spence et al.*, 2013]. The variations in drift period apparent in this figure (e.g., at 20:36 to 21:00 UTC) depend both on electron energy and the spatial variation of $|B|$ as Probe A moves outward to a greater radial distance.

2.4. Dual-Spacecraft Observations

Afforded by the Van Allen Probes provide a unique viewpoint of shock effects as functions of time, L, and energy. During the 8 October event, Probe A follows Probe B across L^* (or L) space by ~1 h with both

©2015. American Geophysical Union. All Rights Reserved.

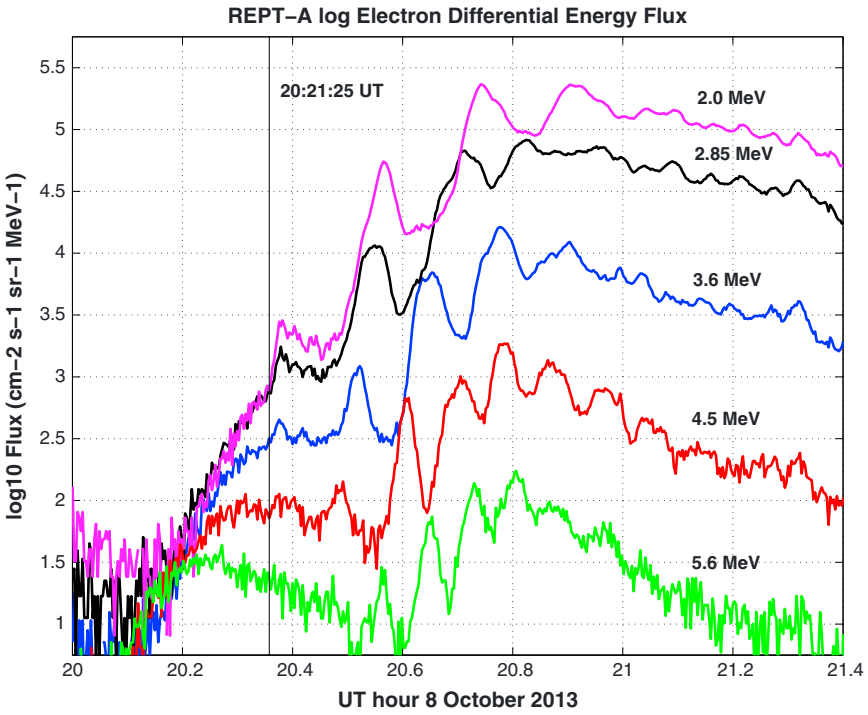

Figure 5. The energy and temporal extent of relativistic electron drift echoes observed by Probe A across several discrete detector channels. The variations in drift period apparent in this figure (e.g., at 20:36 to 21:00 UTC) depend both on electron energy and the spatial variation of $|B|$ as Probe A moves outward to a greater radial distance.

spacecraft traversing essentially the same orbital path. Figure 6 presents an overlay of the Probe A and Probe B L^* profiles of 3.6 MeV REPT electron energy flux along the outbound orbits during which the shock effects were observed. The arrows indicate the 20:22 UT of shock observation at each spacecraft. At shock time, Probe B was at $L^* \sim 5$, and Probe A was further inward near $L^* \sim 3.3$. With this orbital configuration, Probe B observed the preshock background for electron flux and phase space density (PSD) out to $L^* \sim 5$ (i.e., prior to its position at 20:22 UT) ~1 h before Probe A observed the postshock conditions across that range of L^*. Both spacecraft observed enhanced fluxes of highly relativistic electrons and an interval of distinct drift echoes following the shock arrival.

3. Prompt Shock-Induced Effects

Figure 7 presents the Probe A phase space density for constant first and second adiabatic invariants ($\mu = 3500$ MeV/G and $K = 0.114\, R_E\, G^{1/2}$) plotted versus L^* for two orbits before the shock encounter (green), for the orbit of Probe A during the shock encounter (red), and for two orbits after the shock encounter (blue). The black curve was observed by Probe B on its outbound orbit during the shock encounter and sampled the background PSD profile ~1 h prior to the Probe A observations at the same value of L^*. We note the good agreement of the black curve with the preshock (green) profiles for $L^* < 5$. (For details of the PSD calculation, see *Boyd et al.* [2014].)

These REPT observations indicate that the shock effects promptly created a new, enhanced relativistic electron population with peak in phase space density (PSD) on the inner radial gradient of the preshock outer radiation belt where the strong drift echo pulses observed by Van Allen Probe A were seen (cf., Figure 6). Under the effects of the shock-induced electric field, the source population electrons $E \times B$ drifted radially inward, conserving the first and second adiabatic invariants and preserving phase space density along their trajectory. Examination of the figure establishes the relationship between the initial seed population and the accelerated population immediately after the shock-induced acceleration. As we have calculated in section 2, these two populations should be related by the physical displacement given by the shock electric field amplitude times its temporal duration. As described in section 2.2, the source population should lie

©2015. American Geophysical Union. All Rights Reserved.

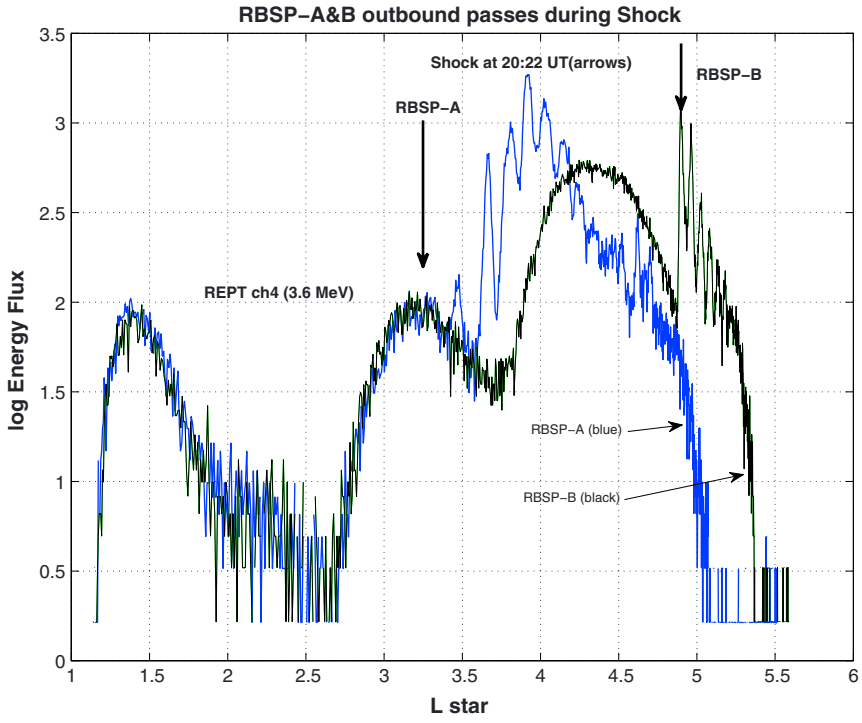

Figure 6. Van Allen Probe A and Probe B L^* profiles of 3.6 MeV REPT electron energy flux are overlaid along the outbound orbits during which the shock effects were observed. The arrows indicate the 20:22 UT of shock observation at each spacecraft. At shock time, Probe B was at L^*~5, and Probe A was further inward near L^*~3.3.

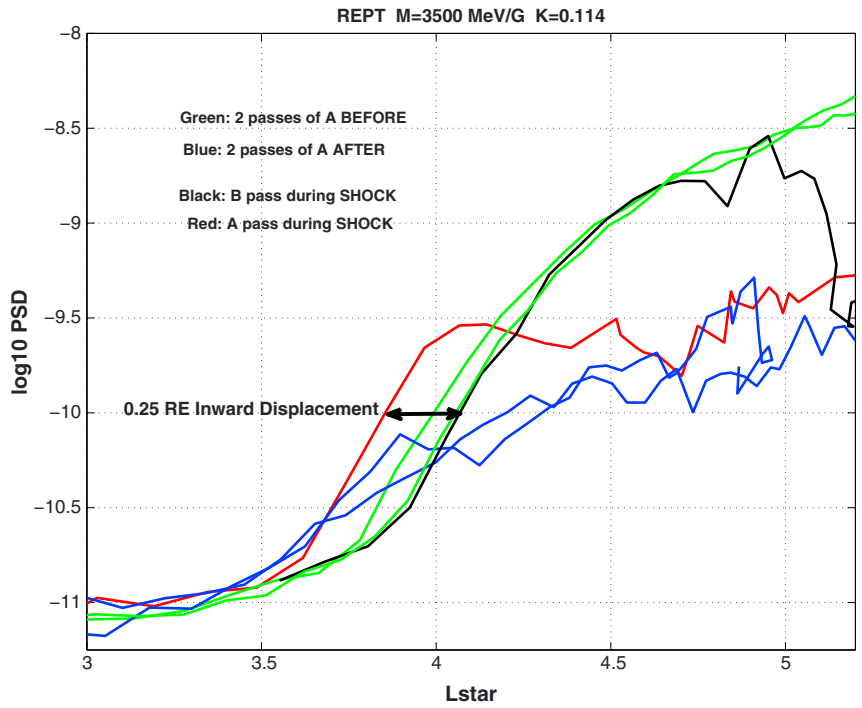

Figure 7. Probe A phase space density for constant first and second adiabatic invariants is plotted versus L^* for two orbits before the shock encounter (green), for the orbit during the shock encounter (red), and for two orbits after the shock encounter (blue). The black curve was observed by Probe B on its outbound orbit during the shock encounter and sampled the background PSD profile ~1 h prior to the Probe A observations at the same value of L^*. Comparison of the red and block profiles indicates an inward displacement of ~0.25 R_E for 4.5 MeV electrons.

©2015. American Geophysical Union. All Rights Reserved.

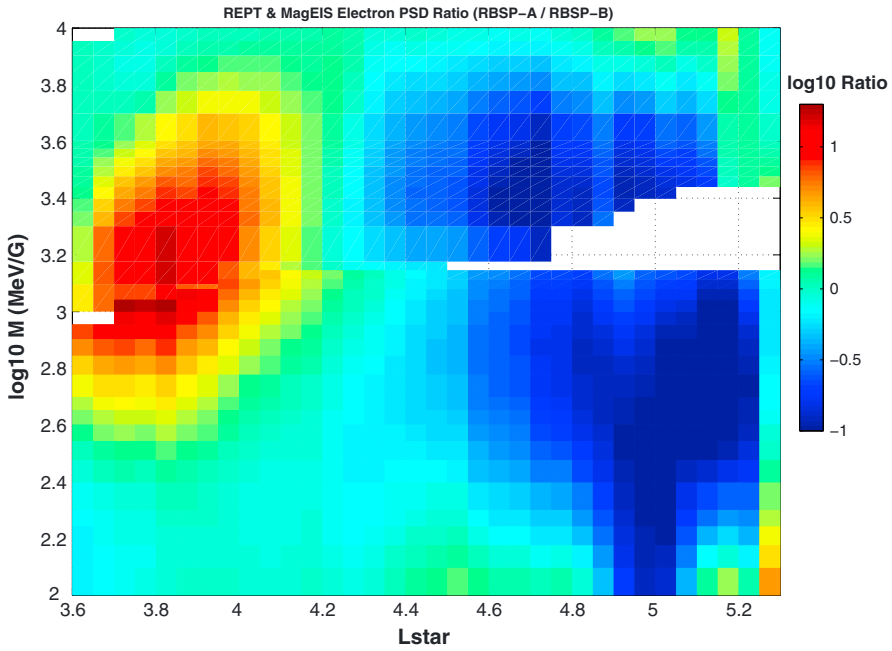

Figure 8. REPT and MagEIS observations are combined to illustrate the change in the electron PSD determined as the ratio of the postshock observations by Probe A to the preshock (background) observations by Probe B. The log10 of the ratio (Probe A PSD/Probe B PSD) for constant K (second invariant) is shown plotted against log μ (first invariant) over a two-decade range of μ from 100 MeV/G to 10,000 MeV/G and for L^* between 3.6 and 5.2.

within about ~0.3 R_E of the accelerated population. This is roughly the offset between the red and the black (Probe B background) PSD profiles and provides a good indication of the source population and its evolution history. Poleward of L^* ~4.2, electron losses due to outward diffusion, and magnetopause shadowing resulted in the significant decrease in PSD and flux seen at higher values of L [*Hudson et al.*, 2015].

We conclude that the enhancement near L^*~3.8 represents a freshly accelerated population of electrons that was not transferred from further out in L adiabatically, i.e., not a population conserving all three invariants. (This is an important check on the shock energization scenario because many of the properties of the energization process are tied to this displacement and to the fact that the first and second adiabatic invariants are conserved.) The prompt nature of the shock-induced energization is constrained by the Van Allen Probe A observation of the PSD enhancement at $L^* = 4$, approximately 15 min following the electric field impulse.

The spatial extent and energy range of the prompt electron acceleration seen during the 8 October 2013 shock event is described in Figure 8, combining observations over the broad range of electron energies observed with the REPT and MagEIS instruments on both Van Allen Probes A and B. During the 1 h prior to the shock arrival, Probe B traversed the range of $L^* = 3.5$ to 5, providing an excellent observation of the unperturbed electron population (cf., Figure 6). Subsequent observations by Probe A across the same extent of L^* sample the postshock electron population as a function of both space and time. Figure 8 presents the change in the electron PSD at each observation point determined as the ratio of the postshock observations by Probe A to the preshock (background) observations by Probe B. The log10 of the ratio (Probe A PSD/Probe B PSD) for constant K (second invariant) is shown, plotted against log μ (first invariant) over a two-decade range of μ from 100 MeV/G to 10,000 MeV/G and for L^* between 3.6 and 5.2. The accelerated population at 1000–5000 MeV/G centered at L^*~3.8 was observed within 20 min of the shock arrival as Probe A traveled outward across that range of L^*. Figure 8 illustrates the promptness ($<$20 min) and both the spatial extent (L^*~3.5 to 4.0) and energy range (2.0 to 5.0 MeV) of the inner region enhancement. This enhanced region remained essentially unchanged in that location for many hours following the shock impact (see Figure 10 below). At higher L^* ($\geq$4.5), significant ($>$10X) loss of the relativistic electron population in the outer regions was observed within ~1 h of the time of shock onset. Radiation belt losses during this and similar events will be treated in a separate publication.

©2015. American Geophysical Union. All Rights Reserved.

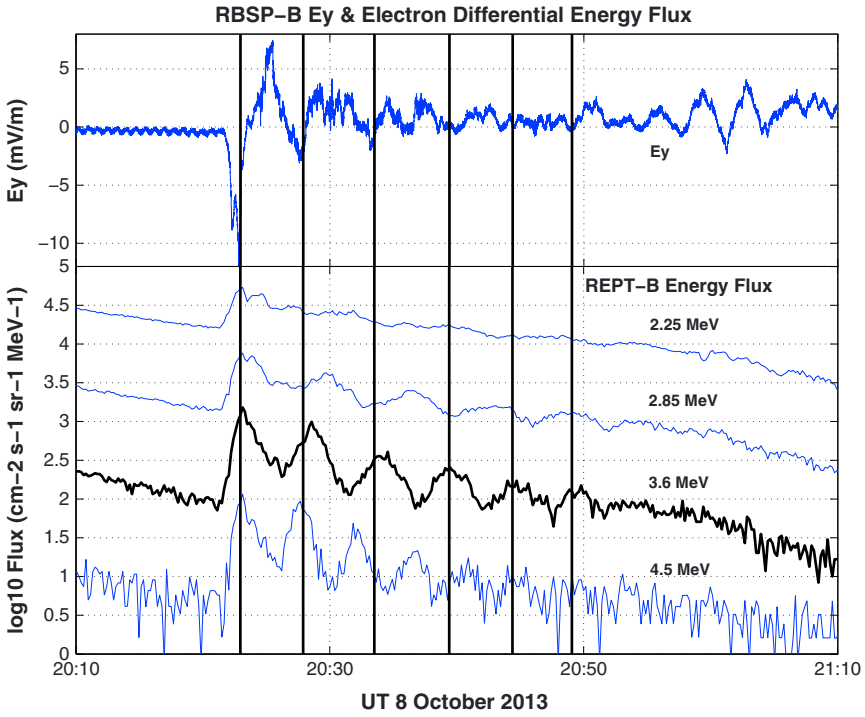

Figure 9. The 3.6 MeV electrons were in drift resonance with a 300 s period ULF wave train that followed the initial shock-induced impulse at the L^*~5 position of Probe B. (top) The Y_{GSE} component of the electric field observed by the EFW instrument. A clear 300 s periodicity is seen in the negative E_y component (vertical black lines). (bottom) REPT differential electron energy flux is plotted for channels 1 through 5 (2.0 MeV through 5.6 MeV).

4. Drift-Resonance Effects

Across a broad range of energies, the entire dayside electron population experiences the accelerating electric field impulse shown in Figure 2. As discussed in section 2.2, the extended (~1 min) duration of the accelerating electric field across a broad extent of the dayside magnetosphere, coupled with energy-dependent gradient drift velocities (cf., Figure 3), selects a preferred range of energies for the resulting initial enhancement ($\delta E/E$) of the outer radiation belt electrons, i.e., those which can stay in the accelerating wave as it propagates tailward. As seen in the Van Allen Probe electric field observations [*Wygant et al.*, 2013] of Figures 2 and 4, the initial accelerating shock impulse was followed by an ~30 min interval of strong ULF oscillations with ~200–400 s period. As the shock-accelerated electrons drift around the Earth, those energies with drift period comparable to ULF wave periods can be resonantly accelerated or decelerated either coherently [*Elkington et al.*, 1999] or by a random walk in the radial direction conserving the first and second invariants [*Fälthammar*, 1968; *Elkington et al.*, 2003, and references therein]. With reference to Figure 3, for the L^*~3.8 center of the strong acceleration region seen in Figure 8, drift-resonant acceleration with the observed ULF waves occurs for relativistic electrons with 2.5 MeV–4 MeV energy. The observed energies of the electrons with a clear drift echo response in Figure 5 have drift periods comparable to the ULF wave periods seen in Figures 2 and 4. These are electrons with μ~1000 MeV/G–4000 MeV/G that correspond to the center of the observed accelerated population (Figure 8).

Figure 9 demonstrates the drift resonance of 3.6 MeV electrons with a 300 s period ULF wave train that followed the initial pulse at the L^*~5 position of Probe B. Figure 9 (top) presents the Y_{GSE} component of the electric field observed by the Electric Field and Waves (EFW) instrument. A clear 300 s periodicity is seen in the negative E_y component (vertical black lines). In Figure 9 (bottom), REPT differential electron energy flux is plotted for channels 2 through 5 (2.25 MeV through 5.6 MeV). Prompt flux enhancements were seen in all energy channels (with largest proportional increases seen at 3.6 MeV and 4.5 MeV—channels 3 and 4), followed by energy-dependent drift echoes. (Probe B was near apogee throughout the interval shown, so there is no significant change in drift echo period due to motion through a changing magnetic field.) At this

©2015. American Geophysical Union. All Rights Reserved.

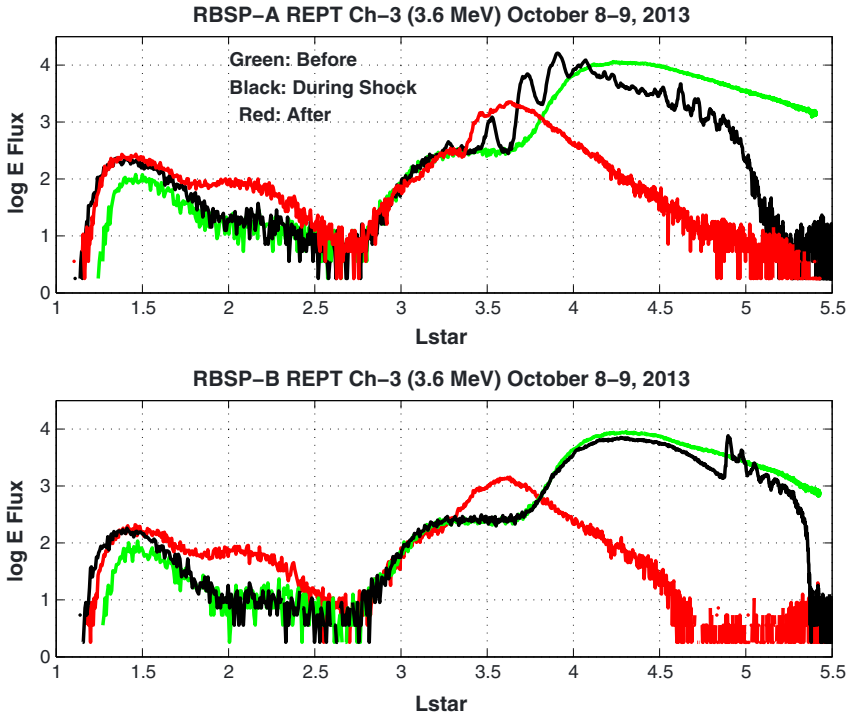

Figure 10. Sequential passes for (top) Probe A and (bottom) Probe B across the outer radiation belt before (green), during (black), and after (red) the shock are presented. The postshock (red) profiles reveal the new population of shock-accelerated electrons that was formed inside L^*~4.

position, the drift period for the electrons in the 3.6 MeV channel closely matches the ULF wave period. The observed peak enhancements of the 3.6 MeV flux align closely with enhancements in negative E_y indicative of drift resonance that may be responsible for additional electron acceleration over multiple electron drift and wave periods.

For strong enough ULF waves with 300 s period, 2.5 MeV resonant electrons at L~6 experiencing $E_y < 0$ on the dayside will be energized and displaced inward. The heavy black arrow in Figure 3 indicates the trajectory taken by an electron that receives exactly enough energy from the wave to remain in resonance with the wave as the electron moves radially inward. (In detail, the frequency of the standing Alfvén waves would increase with increasing $|B|$ at lower values of L, but the description above suffices for the first-order analysis presented here.) If too much energy is received, the electron falls out of resonance with the wave and gives up energy, falling back to the resonance position. If it receives too little, it falls out of resonance and remains at constant L. For an electron following the path of the black arrow, significantly larger energy gain might be achieved ($>$2 MeV) than from the energization associated with the initial shock-induced impulse ($\leq$500 keV).

5. Residual Enhancement

The preceding sections have described the promptness ($<$20 min), energy range (1.5–4.5 MeV), and spatial extent (L^* ~3.5–4.0) of the enhancement of relativistic electrons observed by the Van Allen Probes in the minutes immediately following the 8 October 2013 shock event. Figure 10 presents the sequential passes for Probe A (top) and Probe B (bottom) across the outer radiation belt before (green), during (black), and after (red) the shock. Subsequent orbits show the persistent nature of the new population of shock-accelerated electrons that was formed inside L^*~4.

6. Conclusions

The spatial separation and excellent energy and pitch angle resolution of the Van Allen Probe observations during the 8 October 2013 solar wind shock event provide new detailed insights into the acceleration of

©2015. American Geophysical Union. All Rights Reserved.

electrons to relativistic energies. In particular, the dual-spacecraft observations and detector characteristics allow conversion to phase space density and mapping of observations at constant first and second invariants, removing adiabatic effects associated with both changing magnetic fields during the storm and rotation of the Earth's dipole axis relative to the orbital plane. Our results demonstrate that prompt acceleration by impulsive shock-induced electric fields and subsequent ULF wave processes comprises a significant mechanism for enhancing relativistic electron populations inside the plasmasphere and the heart of the outer zone.

The energy gain and L^* value of enhanced PSD is a function of the electric field amplitude. Thus, the 24 March 1991 event observed on the nightside by CRRES produced a "new belt" of 15 MeV electrons at L~2.5 with an inferred dayside electric field amplitude of ~200 mV/m. In the present study, we are able, with two dayside Van Allen Probes spacecraft, to confirm that the observed ~10 mV/m electric field impulse, present over a longitudinal extent consistent with dual-spacecraft measurements, could transport the measured source population inward to produce the observed peak in flux and PSD at L^*~3.5. This mechanism occurs on an electron drift time scale of minutes immediately following shock arrival, producing a peak in PSD at a comparable location to the local acceleration seen in other CME shock events observed by the Van Allen Probes [*Reeves et al.*, 2013; *Thorne et al.*, 2013] and in simulations [e.g., *Li et al.*, 1993]. A key ingredient for the shock acceleration mechanism is the presence of a robust source population of multi-MeV electrons on the outer edge of the outer zone that can experience drift resonance. A preceding CME shock-driven storm at the beginning of October 2013 produced the source population for the 8 October event.

Acknowledgments
Work at MIT Haystack Observatory was supported by a Van Allen Probes subaward from the University of Minnesota to the Massachusetts Institute of Technology. Work at the University of Colorado and University of New Hampshire was supported by RBSP-ECT funding provided by JHU/APL contract 967399 under NASA's Prime contract NAS5-01072. All Van Allen Probes data used are publicly available at www.rbsp-ect.lanl.gov.

Michael Balikhin thanks the reviewers for their assistance in evaluating this paper.

References

Araki, T., et al. (1997), Anomalous sudden commencement on March 24, 1991, *J. Geophys. Res.*, *102*(A7), 14,075–14,086, doi:10.1029/96JA03637.

Baker, D. N., S. G. Kanekal, X. Li, S. P. Monk, J. Goldstein, and J. L. Burch (2004), An extreme distortion of the Van Allen belt arising from the "Halloween" solar storm in 2003, *Nature*, *432*(7019), 878–881, doi:10.1038/nature03116.

Baker, D. N., et al. (2012), The Relativistic Electron-Proton Telescope (REPT) instrument on board the Radiation Belt Storm Probes (RBSP) spacecraft: Characterization of Earth's radiation belt high-energy particle populations, *Space Sci. Rev.*, doi:10.1007/s11214-012-9950-9.

Baker, D. N., et al. (2013), A long-lived relativistic electron storage ring embedded in Earth's outer Van Allen belt, *Science*, *340*(6129), 186–190, doi:10.1126/science.1233518.

Baker, D. N., et al. (2014), Gradual diffusion and punctuated phase space density enhancements of highly relativistic electrons: Van Allen Probes observations, *Geophys. Res. Lett.*, *41*, 1351–1358, doi:10.1002/2013GL058942.

Blake, J. B., W. A. Kolasinski, R. W. Fillius, and E. G. Mullen (1992), Injection of electrons and protons with eneergies of 10 s of MeV into $L < 3$ on March 24, 1991, *Geophys. Res. Lett.*, *19*, 821–824, doi:10.1029/92GL00624.

Blake, J. B., et al. (2013), Magnetic Electron Ion Spectrometer (MagEIS) instruments aboard the Radiation Belt Storm Probes (RBSP) spacecraft, *Space Sci. Rev.*, doi:10.1007/s11214-013-9991-8.

Boyd, A. J., H. E. Spence, S. G. Claudepierre, J. F. Fennell, J. B. Blake, D. N. Baker, G. D. Reeves, and D. L. Turner (2014), Quantifying the radiation belt seed population in the March 17, 2013 electron acceleration event, *Geophys. Res. Lett.*, *41*, 2275–2281, doi:10.1002/2014GL059626.

Claudepierre, S. G., et al. (2013), Van Allen Probes observation of drift resonance between poloidal mode ultralow frequency waves and 60 keV electrons, *Geophys. Res. Lett.*, *40*, 4491–4497, doi:10.1002/grl.50901.

Elkington, S. R., M. K. Hudson, and A. A. Chan (1999), Acceleration of relativistic electrons via drift-resonant interaction with toroidal-mode Pc-5 ULF oscillations, *Geophys. Res. Lett*, *26*(21), 3273–3276, doi:10.1029/1999GL003659.

Elkington, S. R., M. K. Hudson, M. J. Wiltberger, and J. G. Lyon (2002), MHD/particle simulations of radiation belt dynamics, *J. Atmos. Sol. Terr. Phys.*, *64*, 607–615.

Elkington, S. R., M. K. Hudson, and A. A. Chan (2003), Resonant acceleration and diffusion of outer zone electrons in an asymmetric geomagnetic field, *J. Geophys. Res.*, *108*(A3), 1116, doi:10.1029/2001JA009202.

Eriksson, P. T. I., L. G. Blomberg, S. Schaefer, and K.-H. Glassmeier (2006), On the excitation of ULF waves by solar wind pressure enhancements, *Ann. Geophys.*, *11*, 3161–3172.

Fälthammar, C.-G. (1968), Radial diffusion by violation of the third adiabatic invariant, in *Earth's Particles and Fields*, edited by B. M. McCormac, p. 157, Reinhold, New York.

Foster, J. C., et al. (2014), Prompt energization of relativistic and highly relativistic electrons during a substorm interval: Van Allen Probes observations, *Geophys. Res. Lett.*, *41*, 20–25, doi:10.1002/2013GL058438.

Gannon, J. L., X. Li, and M. Temerin (2005), Parametric study of shock-induced transport and energization of relativistic electrons in the magnetosphere, *J. Geophys. Res.*, *110*, A12206, doi:10.1029/2004JA010679.

Hudson, M. K., S. R. Elkington, J. G. Lyon, V. A. Marchenko, I. Roth, M. Temerin, J. B. Blake, M. S. Gussenhoven, and J. R. Wygant (1997), Simulations of radiation belt formation during storm sudden commencements, *J. Geophys. Res.*, *102*(A7), 14,087–14,102, doi:10.1029/97JA03995.

Hudson, M. K., R. E. Denton, M. R. Lessard, E. G. Miftakhova, and R. R. Anderson (2004), A study of Pc-5 ULF oscillations, *Ann. Geophys.*, *22*, 289–302, doi:10.5194/angeo-22-289-2004.

Hudson, M. K., J. Paral, B. T. Kress, M. Wiltberger, D. N. Baker, J. C. Foster, D. L. Turner, and J. R. Wygant (2015), Modeling CME-shock driven storms in 2012–2013: MHD test particle simulations, *J. Geophys. Res. Space Physics*, *120*, doi:10.1002/2014JA020833, in press.

Kress, B. T., M. K. Hudson, M. D. Looper, J. Albert, J. G. Lyon, and C. C. Goodrich (2007), Global MHD test particle simulations of >10 MeV radiation belt electrons during storm sudden commencement, *J. Geophys. Res.*, *112*, A09215, doi:10.1029/2006JA012218.

Li, X., I. Roth, M. Temerin, J. R. Wygant, M. K. Hudson, and J. B. Blake (1993), Simulation of the prompt energization and transport of radiation belt particles during the March 24, 1991 SSC, *Geophys. Res. Lett.*, *20*(22), 2423–2426, doi:10.1029/93GL02701.

©2015. American Geophysical Union. All Rights Reserved.

Mann, I. R., et al. (2013), Discovery of the action of a geophysical synchrotron in the Earth's Van Allen radiation belts, *Nat. Commun.*, *4*, 2795, doi:10.1038/ncomms3795.

Mauk, B. H., et al. (2012), Science objectives and rationale for the Radiation Belt Storm Probe mission, *Space Sci. Rev.*, doi:10.1007/s11214-012-9908-y.

Reeves, G. D., et al. (2013), Electron acceleration in the heart of the Van Allen radiation belts, *Science*, doi:10.1126/science.1237743.

Roederer, J. (1970), *Dynamics of Geomagnetically Trapped Radiation*, Springer, New York.

Schulz, M., and L. J. Lanzerotti (1974), *Particle Diffusion in the Radiation Belts*, Springer, New York.

Spence, H. E., et al. (2013), Science goals and overview of the Radiation Belt Storm Probes (RBSP) Energetic Particle, Composition, and Thermal Plasma (ECT) Suite on NASA's Van Allen Probe mission, *Space Sci. Rev.*, doi:10.1007/s11214-013-0007-5.

Tan, L. C., X. Shao, A. S. Sharma, and S. F. Fung (2011), Relativistic electron acceleration by compressional-mode ULF waves: Evidence from correlated Cluster, Los Alamos National Laboratory spacecraft, and ground-based magnetometer measurements, *J. Geophys. Res.*, *116*, A07226, doi:10.1029/2010JA016226.

Thorne, R. M., et al. (2013), Rapid local acceleration of relativistic radiation-belt electrons by magnetospheric chorus, *Nature*, *504*, 411–414, doi:10.1038/nature12889.

Tsyganenko, N. A., and M. I. Sitnov (2005), Modeling the dynamics of the inner magnetosphere during strong geomagnetic storms, *J. Geophys. Res.*, *110*, A03208, doi:10.1029/2004JA010798.

Turner, D. L., et al. (2014), Competing source and loss mechanisms from wave-particle interactions in Earth's outer radiation belt during the 30 Sep to 03 Oct 2012 geomagnetic storm, *J. Geophys. Res. Space Physics*, *119*, 1960–1979, doi:10.1002/2014JA019770.

Wygant, J. R., et al. (2013), The Electric Field and Waves (EFW) instruments on the Radiation Belt Storm Probe mission, *Space Sci. Rev.*, doi:10.1007/s1124-013-0013-7.

Wygant, J., F. Mozer, M. Temerin, J. Blake, N. Maynard, H. Singer, and M. Smiddy (1994), Large amplitude electric and magnetic field signatures in the inner magnetosphere during injection of 15 MeV electron drift echoes, *Geophys. Res. Lett.*, *21*, 1739–1742, doi:10.1029/94GL00375.

Zong, Q.-G., et al. (2009), Vortex-like plasma flow structures observed by Cluster at the boundary of the outer radiation belt and ring current: A link between the inner and outer magnetosphere, *J. Geophys. Res.*, *114*, A10211, doi:10.1029/2009JA014388.

©2015. American Geophysical Union. All Rights Reserved.